Acta Cryst E CRYSTALLOGRAPHIC COMMUNICATIONS

ISSN 2056-9890

Crystal structure and Hirshfeld surface analyses, interaction energy calculations and energy frameworks of 2-(anthracen-10-yl)-1*H*-benzo[*d*]-imidazole

Naser E. Eltayeb,[a,b] Yaseen A. Almehmadi,[a,c] Tuncer Hökelek,[d] Jamal Lasri[a]* and Aidan P. McKay[e]

[a]Department of Chemistry, Rabigh College of Science and Arts, King Abdulaziz University, Jeddah 21589, Saudi Arabia, [b]Department of Chemistry, Faculty of Pure and Applied Sciences, International University of Africa, Khartoum 2469, Sudan, [c]King Fahd Medical Research Center, King Abdulaziz University, Jeddah 21589, Saudi Arabia, [d]Department of Physics, Hacettepe University, 06800 Beytepe, Ankara, Türkiye, and [e]EaStCHEM School of Chemistry, University of St Andrews, Fife KY16 9ST, United Kingdom. *Correspondence e-mail: jlasri@kau.edu.sa

Received 9 December 2025
Accepted 23 December 2025

Edited by L. Van Meervelt, Katholieke Universiteit Leuven, Belgium

Keywords: 2-(anthracen-10-yl)-1*H*-benzo[*d*]imidazole; crystal structure; hydrogen bond; π-stacking; Hirshfeld surface.

CCDC reference: 2518388

Supporting information: this article has supporting information at journals.iucr.org/e

The benzimidazole and anthracene moieties in the title compound, $C_{21}H_{14}N_2$, are oriented at a dihedral angle of 46.00 (2)°. In the crystal, N—H···N hydrogen bonds link the molecules into infinite chains along the *b*-axis direction. In addition, C—H···π interactions contribute to the consolidation of the packing. A Hirshfeld surface analysis of the crystal structure indicates that the most important contributions to the crystal packing are from H···H (47.2%) and H···/C···H (39.4%) interactions. An energy-framework calculation indicates that the electrostatic and dispersion energies are the most important contributors to the packing.

1. Chemical context

Benzimidazole, a nitrogen-containing aromatic heterocycle, is a key component in different biologically active molecules (Bansal & Silakari, 2012) encompassing a broad spectrum of activities, including anticancer (Chen *et al.*, 2010; Sontakke *et al.*, 2015), antiviral (Li *et al.*, 2006), antimicrobial (Sharma *et al.*, 2009) and antifungal (Goker *et al.*, 2002) activities. Different chemotherapeutic anticancer drugs interact directly with DNA or prevent the appropriate relaxation of DNA through inhibition of topoisomerases (Chen & Liu, 1994). Currently, our research work focuses on the synthesis, characterization and anticancer evaluation of a variety of acyclic and cyclic imine-type compounds (Eltayeb *et al.*, 2020*a*,*b*, 2025; Lasri *et al.*, 2018, 2023*a*,*b*, 2024, 2025). Herein we report the synthesis, molecular and crystal structure, Hirshfeld surface analysis, interaction energy calculations and energy frameworks of the title compound (I).

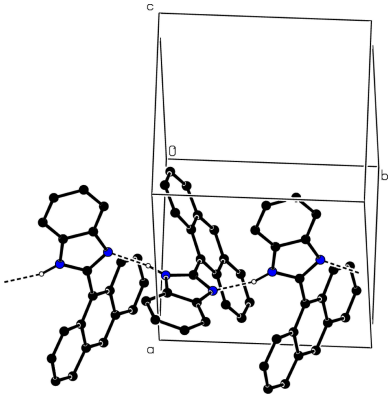

2. Structural commentary

The title compound contains benzimidazole and anthracene ring systems (Fig. 1). The benzimidazole moiety is essentially planar [r.m.s. deviation = 0.013 (1) Å] with a maximum deviation of 0.0195 (12) Å for atom C5. In the anthracene moiety, the almost planar *A* (C11–C16), *B* (C10/C11/C16–C18/C23) and *C* (C18–C23) rings are oriented at dihedral angles of *A*/*B* = 2.48 (4)°, *A*/*C* = 5.67 (4)° and *B*/*C* = 3.20 (4)° and are thus nearly coplanar. The dihedral angle between the mean planes of the benzimidazole and anthracene ring

systems is 46.00 (2)°. There are no unusual bond lengths or interbond angles in the molecule.

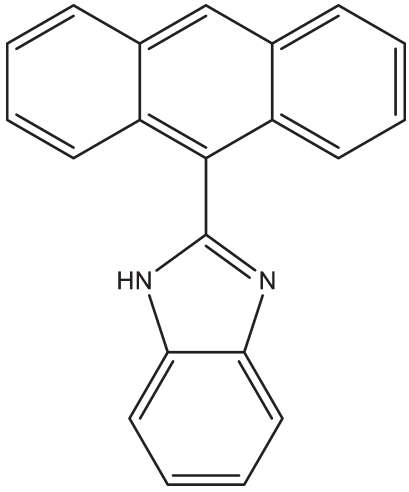

.

3. Supramolecular features

In the crystal, N—H···N hydrogen bonds (Table 1) link the molecules into infinite chains along the *b*-axis direction (Fig. 2). The C—H···π interactions (Table 1) help to consolidate the crystal packing. Despite the presence of aromatic rings, there are no π–π stacking interactions. The shortest centroid-to-centroid distances are 4.1943 (7) Å [for the *A* and *B* rings, α = 32.09 (3)°], 4.3273 (7) Å [for the (C3–C8) and *C* rings, α = 43.98 (4)°] and 4.4415 (7) Å [for the (N2/N9/C1/C3/C8) and *C* rings, α = 44.82 (4)°].

A Hirshfeld surface (HS) analysis was carried out using *Crystal Explorer 17.5* (Spackman *et al.*, 2021) to clarify the intermolecular interactions in (I). The Hirshfeld surface plotted over d_{norm} is shown in Fig. 3, where the bright-red spots correspond to the respective donors and/or acceptors;

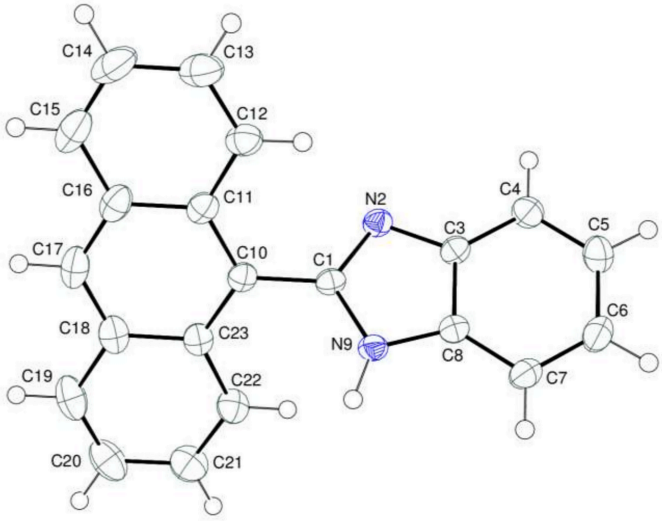

Figure 1
Molecular structure of the title molecule with atom-numbering scheme and 50% probability ellipsoids.

Table 1
Hydrogen-bond geometry (Å, °).

*Cg*1, *Cg*2, *Cg*3 and *Cg*4 are the centroids of the (N2/N9/C1/C3–C8), (C10/C11/C16–C21), (C10/C11/C16–C18,C23) and (C3–C8) rings, respectively.

D—H···*A*	*D*—H	H···*A*	*D*···*A*	*D*—H···*A*
N9—H9···N2^{i}	0.95 (1)	1.92 (1)	2.8186 (13)	157 (1)
C5—H5···*Cg*1^{iii}	0.95	2.96	3.8219 (12)	151
C13—H13···*Cg*2^{iv}	0.95	2.97	3.4156 (14)	110
C20—H20···*Cg*3^{i}	0.95	2.90	3.5625 (16)	128
C21—H21···*Cg*4^{v}	0.95	2.75	3.2887 (15)	116

Symmetry codes: (i) $-x+\frac{3}{2}, y+\frac{1}{2}, z$; (iii) $x+\frac{1}{2}, y, -z+\frac{3}{2}$; (iv) $-x+\frac{3}{2}, y-\frac{1}{2}, z$; (v) $x-1, y, z$.

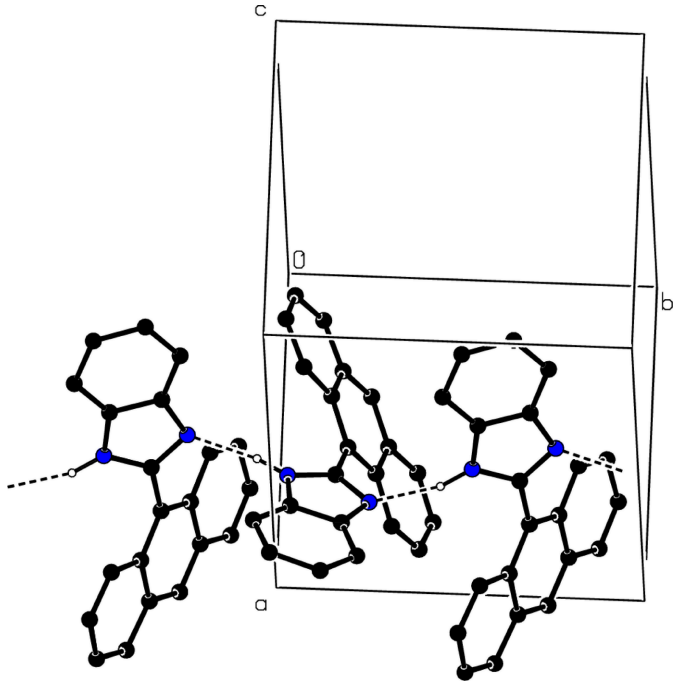

Figure 2
A partial packing diagram of the title compound. Intermolecular N—H···N hydrogen bonds are shown as dashed lines. H atoms not involved in these interactions have been omitted for clarity.

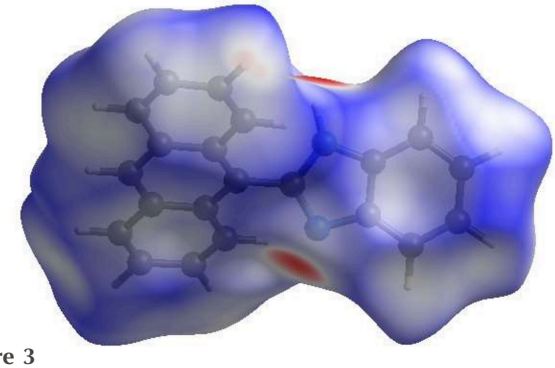

Figure 3
View of the three-dimensional Hirshfeld surface of the title compound plotted over d_{norm}.

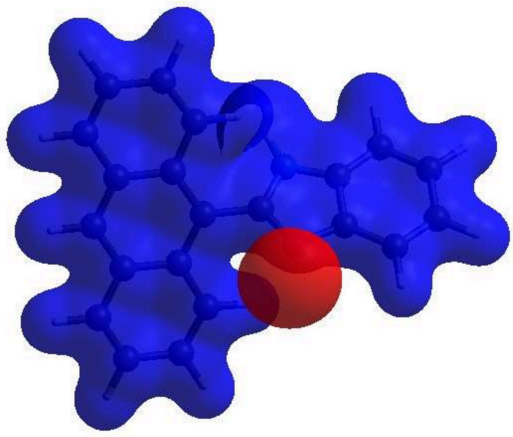

Figure 4
View of the Hirshfeld surface of the title compound plotted over electrostatic potential energy using the STO-3 G basis set at the Hartree–Fock level of theory. Hydrogen-bond donors and acceptors are shown as blue and red regions around the atoms corresponding to positive and negative potentials, respectively.

they also appear as blue and red regions in Fig. 4 corresponding to positive and negative potentials (Spackman *et al.*, 2008). The absence of π–π stacking interactions is indicated by the absence of the adjacent red and blue triangles in the rings (Fig. 5*a* and *b*). On the other hand, the C—H$\cdots\pi$ interactions (Table 1) are represented as red π-holes, which are related to the electron ring interactions between C—H groups with the centroid of the *B* (C3–C8) and *C* (C10/C11/C16–C18/C23) rings of neighbouring molecules (Fig. 5*a* and *b*). According to the two-dimensional fingerprint plots (McKinnon *et al.*, 2007), the intermolecular H$\cdots$H and H$\cdots$C/C$\cdots$H (Table 2) contacts make the most important contributions to the HS (47.2% and 39.8%, respectively) (Fig. 6).

4. Interaction energy calculations and energy frameworks

The CE–B3LYP/6–31G(d,p) energy model available in *Crystal Explorer 17.5* (Spackman *et al.*, 2021) was used to calculate the intermolecular interaction energies. Hydrogen-bonding interaction energies (in kJ mol^{-1}) for N9—H9$\cdots$N2 were calculated to be −57.9 (E_{ele}), −16.4 (E_{pol}), −60.9 (E_{dis}), 86.9 (E_{rep}) and −72.7 (E_{tot}). Energy frameworks combine the calculation of intermolecular interaction energies with a graphical representation of their magnitude (Turner *et al.*, 2015). Energy frameworks were constructed for E_{ele} (red cylinders), E_{dis} (green cylinders) and E_{tot} (blue cylinders) (Fig. 7*a*, *b* and *c*), and their evaluation indicates that the stabilization is dominated equally *via* the electrostatic and dispersion energy contributions in the crystal structure of (I).

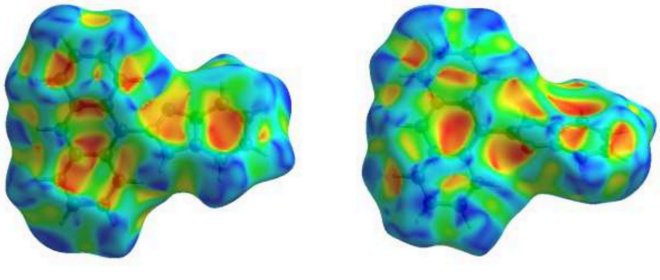

(a) (b)

Figure 5
Hirshfeld surface of the title compound for two orientations plotted over shape-index.

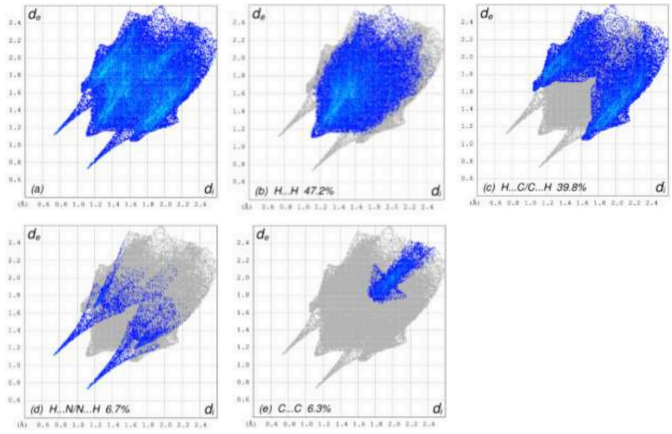

Figure 6
The full two-dimensional fingerprint plots for the title compound, showing (*a*) all interactions, and delineated into (*b*) H$\cdots$H, (*c*) H$\cdots$C/C$\cdots$H, (*d*) H$\cdots$N/N$\cdots$H and (*e*) C$\cdots$C interactions. The d_i and d_e values are the closest internal and external distances (in Å) from given points on the Hirshfeld surface.

5. Synthesis and crystallization

To a solution of 9-anthracenecarboxaldehyde (206.2 mg, 1.0 mmol) in ethanol (50 ml) was added 1,2-phenylenediamine (108.1 mg, 1.0 mmol) and the reaction mixture was refluxed for 4 h. The reaction was cooled to room temperature for precipitation, and then filtered. Yellow crystals suitable for X-ray analysis were obtained by slow evaporation of an ethanol solution. Yield: 70%. M.p. 534–536 K. IR (cm^{-1}): 1227, 1401, 1619, 2917, 3050. ^{1}H NMR (DMSO-d_6): δ 7.31 (*s*, 2H), 7.50 (*m*, 4H), 7.71 (*d*, *J* = 8.1 Hz, 4H), 8.18 (*d*, *J* = 7.2 Hz, 2H), 8.79 (*s*, 1H), 13.02 (*bs*, 1H). ^{13}C NMR (DMSO-d_6): δ 121.9, 125.4, 125.6, 126.6, 128.3, 128.7, 130.4, 130.5, 149.4.

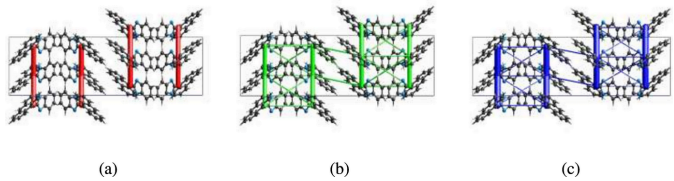

(a) (b) (c)

Figure 7
The energy frameworks for a cluster of molecules of the title compound viewed down the *a*-axis showing the (*a*) electrostatic energy, (*b*) dispersion energy and (*c*) total energy diagrams. The cylindrical radius is proportional to the relative strength of the corresponding energies and they were adjusted to the same scale factor of 80 with cut-off value of 5 kJ mol^{-1} within 2 × 2 × 2 unit cells.

Elemental analysis calculated for $C_{21}H_{14}N_2$ (294.36), C, 85.69; H, 4.79; N, 9.52%. Found: C, 85.68, H, 4.77, N, 9.51%. This compound has been previously synthesized by Sontakke *et al.* (2015) and Barwiolek *et al.* (2019).

6. Refinement

Crystal data, data collection and structure refinement details are summarized in Table 2. The N-bound H atom was located in a difference Fourier map and was refined isotropically. The C-bound H atoms were calculated geometrically at a distance of 0.95 Å (for aromatic CH) and refined using a riding model by applying the constraint $U_{iso}(H) = 1.2U_{eq}(C)$.

Acknowledgements

The authors would like to thank D. B. Cordes for his fruitful discussion. TH is grateful to Hacettepe University Scientific Research Project Unit.

Funding information

Funding for this research was provided by: Hacettepe Üniversitesi (grant No. 013 D04 602 004).

Table 2
Experimental details.

Crystal data	
Chemical formula	$C_{21}H_{14}N_2$
M_r	294.34
Crystal system, space group	Orthorhombic, *Pbca*
Temperature (K)	173
a, *b*, *c* (Å)	8.30341 (17), 9.5845 (2), 37.0413 (8)
V (Å^3)	2947.90 (11)
Z	8
Radiation type	Mo *Kα*
μ (mm^{-1})	0.08
Crystal size (mm)	0.11 × 0.10 × 0.01
Data collection	
Diffractometer	Rigaku XtaLAB P200K
Absorption correction	Multi-scan (*CrysAlis PRO*; Rigaku OD, 2024)
T_{min}, T_{max}	0.854, 1.000
No. of measured, independent and observed [$I > 2\sigma(I)$] reflections	59653, 3810, 3005
R_{int}	0.039
(sin $\theta/\lambda)_{max}$ (Å^{-1})	0.698
Refinement	
$R[F^2 > 2\sigma(F^2)]$, $wR(F^2)$, *S*	0.041, 0.103, 1.05
No. of reflections	3810
No. of parameters	212
No. of restraints	1
H-atom treatment	H atoms treated by a mixture of independent and constrained refinement
$\Delta\rho_{max}$, $\Delta\rho_{min}$ (e Å^{-3})	0.23, −0.22

Computer programs: *CrysAlis PRO* (Rigaku OD, 2024), *SHELXT2018/2* (Sheldrick, 2015*a*), *SHELXL2019/3* (Sheldrick, 2015*b*) and *OLEX2* (Dolomanov *et al.*, 2009).

References

Bansal, Y. & Silakari, O. (2012). *Bioorg. Med. Chem.* **20**, 6208–6236.
Barwiolek, M., Wojtczak, A., Kozakiewicz, A., Babinska, M., Tafelska-Kaczmarek, A., Larsen, E. & Szlyk, E. (2019). *J. Lumin.* **211**, 88–95.
Chen, A. Y. & Liu, L. F. (1994). *Annu. Rev. Pharmacol. Toxicol.* **34**, 191–218.
Chen, J., Wang, Z., Li, C. M., Lu, Y. P., Vaddady, K., Meibohm, B., Dalton, J. T., Miller, D. D. & Li, W. (2010). *J. Med. Chem.* **53**, 7414–7427.
Dolomanov, O. V., Bourhis, L. J., Gildea, R. J., Howard, J. A. K. & Puschmann, H. (2009). *J. Appl. Cryst.* **42**, 339–341.
Eltayeb, N. E., Hökelek, T. & Lasri, J. (2025). *Acta Cryst.* E**81**, 595–599.
Eltayeb, N. E., Lasri, J., Soliman, S. M., Mavromatis, C., Hajjar, D., Elsilk, S. E., Babgi, B. A. & Hussien, M. A. (2020*b*). *J. Mol. Struct.* **1213**, 128185.
Eltayeb, N. E., Şen, F., Lasri, J., Hussien, M. A., Elsilk, S. E., Babgi, B. A., Gökçe, H. & Sert, Y. (2020*a*). *J. Mol. Struct.* **1202**, 127315.
Göker, H., Kuş, C., Boykin, D. W., Yildiz, S. & Altanlar, N. (2002). *Bioorg. Med. Chem.* **10**, 2589–2596.
Lasri, J., Aly, M. M., Eltayeb, N. E. & Babgi, B. A. (2018). *J. Mol. Struct.* **1164**, 1–8.
Lasri, J., Eltayeb, N. E., Soliman, S. M., Ali, E. M. M., Adam, A. M., Roe, S. M., Akhdhar, A., Alzahrani, F. A., Alshhikh, N. E. & Babgi, B. A. (2025). *ChemistrySelect* **10**, e01452.
Lasri, J., Eltayeb, N. E., Soliman, S. M., Ali, E. M. M., Alhayyani, S. & Akhdhar, A. (2023*a*). *Molecules* **28**, 4766.
Lasri, J., Eltayeb, N. E., Soliman, S. M., Ali, E. M. M., Alhayyani, S., Akhdhar, A. & Hussien, M. A. (2023*b*). *J. Mol. Struct.* **1287**, 135673.
Lasri, J., Eltayeb, N. E., Soliman, S. M., Ali, E. M. M., Rosli, M. M., Alzahrani, F. A., Eid, T. M., Alhayyani, S., Akhdhar, A., Dutta, A., Jaremko, M., Emwas, A. H. & Almaqwashi, A. A. (2024). *ChemistrySelect* **9**, e202402236.
Li, Y. F., Wang, G. F., He, P. L., Huang, W. G., Zhu, F. H., Gao, H. Y., Tang, W., Luo, Y., Feng, C. L., Shi, L. P., Ren, Y. D., Lu, W. & Zuo, J. P. (2006). *J. Med. Chem.* **49**, 4790–4794.
McKinnon, J. J., Jayatilaka, D. & Spackman, M. A. (2007). *Chem. Commun.* pp. 3814–3816.
Rigaku OD (2024). *CrysAlis PRO*. Rigaku Oxford Diffraction, Yarnton, England.
Sharma, D., Narasimhan, B., Kumar, P. & Jalbout, A. (2009). *Eur. J. Med. Chem.* **44**, 1119–1127.
Sheldrick, G. M. (2015*a*). *Acta Cryst.* A**71**, 3–8.
Sheldrick, G. M. (2015*b*). *Acta Cryst.* C**71**, 3–8.
Sontakke, V. A., Kate, A. N., Ghosh, S., More, P., Gonnade, R., Kumbhar, N. M., Kumbhar, A. A., Chopade, B. A. & Shinde, V. S. (2015). *New J. Chem.* **39**, 4882–4890.
Spackman, M. A., McKinnon, J. J. & Jayatilaka, D. (2008). *CrystEngComm* **10**, 377–388.
Spackman, P. R., Turner, M. J., McKinnon, J. J., Wolff, S. K., Grimwood, D. J., Jayatilaka, D. & Spackman, M. A. (2021). *J. Appl. Cryst.* **54**, 1006–1011.
Turner, M. J., Thomas, S. P., Shi, M. W., Jayatilaka, D. & Spackman, M. A. (2015). *Chem. Commun.* **51**, 3735–3738.

supporting information

Acta Cryst. (2026). E**82**, 187-190 [https://doi.org/10.1107/S2056989025011594]

Crystal structure and Hirshfeld surface analyses, interaction energy calculations and energy frameworks of 2-(anthracen-10-yl)-1*H*-benzo[*d*]imidazole

Naser E. Eltayeb, Yaseen A. Almehmadi, Tuncer Hökelek, Jamal Lasri and Aidan P. McKay

Computing details

2-(anthracen-10-yl)-1*H*-benzo[*d*]imidazole

Crystal data

$C_{21}H_{14}N_2$
M_r = 294.34
Orthorhombic, *Pbca*
a = 8.30341 (17) Å
b = 9.5845 (2) Å
c = 37.0413 (8) Å
V = 2947.90 (11) Å^3
Z = 8
F(000) = 1232
D_x = 1.326 Mg m^{-3}
Mo *Kα* radiation, *λ* = 0.71073 Å
Cell parameters from 23539 reflections
θ = 2.2–28.5°
μ = 0.08 mm^{-1}
T = 173 K
Plate, yellow
0.11 × 0.1 × 0.01 mm

Data collection

Rigaku XtaLAB P200K diffractometer
Radiation source: Rotating Anode, Rigaku FR-X
Rigaku Osmic Confocal Optical System monochromator
Detector resolution: 5.8140 pixels mm^{-1}
shutterless scans
Absorption correction: multi-scan (CrysAlisPro; Rigaku OD, 2024)
T_{min} = 0.854, T_{max} = 1.000
59653 measured reflections
3810 independent reflections
3005 reflections with $I > 2\sigma(I)$
R_{int} = 0.039
θ_{max} = 29.7°, θ_{min} = 2.2°
h = −10→11
k = −11→12
l = −49→50

Refinement

Refinement on F^2
Least-squares matrix: full
$R[F^2 > 2\sigma(F^2)]$ = 0.041
$wR(F^2)$ = 0.103
S = 1.05
3810 reflections
212 parameters
1 restraint
Primary atom site location: dual
Hydrogen site location: mixed
H atoms treated by a mixture of independent and constrained refinement
$w = 1/[\sigma^2(F_o^2) + (0.0444P)^2 + 0.8465P]$ where $P = (F_o^2 + 2F_c^2)/3$
$(\Delta/\sigma)_{max}$ = 0.001
$\Delta\rho_{max}$ = 0.23 e Å^{-3}
$\Delta\rho_{min}$ = −0.22 e Å^{-3}

Special details

Geometry. All esds (except the esd in the dihedral angle between two l.s. planes) are estimated using the full covariance matrix. The cell esds are taken into account individually in the estimation of esds in distances, angles and torsion angles; correlations between esds in cell parameters are only used when they are defined by crystal symmetry. An approximate (isotropic) treatment of cell esds is used for estimating esds involving l.s. planes.

Refinement. Hydrogen atom on N9 was located from the F_{map} and refined isotropically with N—H distance restrained to 0.98 Å

Fractional atomic coordinates and isotropic or equivalent isotropic displacement parameters (Å²)

	x	*y*	*z*	U_{iso}*/U_{eq}
N2	0.84627 (11)	0.24750 (9)	0.66012 (2)	0.0248 (2)
N9	0.77061 (11)	0.47141 (9)	0.66026 (2)	0.0242 (2)
H9	0.7166 (17)	0.5562 (14)	0.6545 (4)	0.047 (4)*
C1	0.75069 (13)	0.34240 (11)	0.64528 (3)	0.0227 (2)
C3	0.93528 (13)	0.31880 (11)	0.68609 (3)	0.0244 (2)
C4	1.05794 (14)	0.27224 (12)	0.70899 (3)	0.0309 (3)
H4	1.092555	0.177772	0.708690	0.037*
C5	1.12702 (15)	0.36837 (13)	0.73207 (3)	0.0354 (3)
H5	1.210908	0.339403	0.747813	0.043*
C6	1.07597 (15)	0.50770 (13)	0.73274 (3)	0.0349 (3)
H6	1.125182	0.570561	0.749220	0.042*
C7	0.95616 (14)	0.55626 (12)	0.71013 (3)	0.0303 (3)
H7	0.922156	0.650883	0.710563	0.036*
C8	0.88755 (13)	0.45913 (11)	0.68660 (3)	0.0241 (2)
C10	0.63824 (13)	0.31325 (11)	0.61517 (3)	0.0247 (2)
C11	0.69459 (14)	0.23639 (11)	0.58494 (3)	0.0281 (2)
C12	0.85679 (16)	0.18867 (12)	0.58106 (3)	0.0340 (3)
H12	0.933298	0.209447	0.599360	0.041*
C13	0.90366 (19)	0.11377 (14)	0.55153 (3)	0.0447 (3)
H13	1.012312	0.083653	0.549572	0.054*
C14	0.7934 (2)	0.08031 (15)	0.52384 (4)	0.0514 (4)
H14	0.826830	0.024926	0.503930	0.062*
C15	0.6404 (2)	0.12719 (14)	0.52571 (3)	0.0470 (4)
H15	0.567928	0.106712	0.506574	0.056*
C16	0.58481 (16)	0.20700 (12)	0.55586 (3)	0.0344 (3)
C17	0.42855 (16)	0.25784 (14)	0.55726 (3)	0.0381 (3)
H17	0.357257	0.237922	0.537875	0.046*
C18	0.37304 (14)	0.33687 (13)	0.58608 (3)	0.0329 (3)
C19	0.21431 (15)	0.39448 (15)	0.58616 (4)	0.0426 (3)
H19	0.145176	0.377682	0.566191	0.051*
C20	0.16066 (15)	0.47227 (16)	0.61405 (4)	0.0447 (3)
H20	0.056231	0.512637	0.613230	0.054*
C21	0.26038 (15)	0.49346 (15)	0.64446 (4)	0.0416 (3)
H21	0.220969	0.546298	0.664275	0.050*
C22	0.41201 (14)	0.43952 (13)	0.64588 (3)	0.0333 (3)
H22	0.475211	0.453120	0.666965	0.040*
C23	0.47781 (13)	0.36291 (11)	0.61628 (3)	0.0275 (2)

Atomic displacement parameters (Å²)

	U^{11}	U^{22}	U^{33}	U^{12}	U^{13}	U^{23}
N2	0.0288 (5)	0.0191 (4)	0.0266 (4)	−0.0012 (4)	−0.0007 (4)	0.0005 (3)
N9	0.0247 (5)	0.0190 (4)	0.0290 (5)	0.0010 (4)	−0.0006 (4)	−0.0015 (4)
C1	0.0237 (5)	0.0191 (5)	0.0254 (5)	−0.0020 (4)	0.0031 (4)	−0.0004 (4)
C3	0.0275 (5)	0.0218 (5)	0.0238 (5)	−0.0018 (4)	0.0017 (4)	0.0000 (4)
C4	0.0351 (6)	0.0277 (6)	0.0300 (6)	0.0025 (5)	−0.0030 (5)	0.0034 (4)
C5	0.0361 (6)	0.0402 (7)	0.0301 (6)	0.0002 (5)	−0.0074 (5)	0.0026 (5)
C6	0.0361 (6)	0.0377 (7)	0.0309 (6)	−0.0049 (5)	−0.0033 (5)	−0.0081 (5)
C7	0.0324 (6)	0.0263 (5)	0.0323 (6)	−0.0019 (5)	0.0015 (5)	−0.0061 (4)
C8	0.0247 (5)	0.0232 (5)	0.0244 (5)	−0.0006 (4)	0.0026 (4)	−0.0002 (4)
C10	0.0284 (5)	0.0198 (5)	0.0259 (5)	−0.0034 (4)	−0.0007 (4)	0.0018 (4)
C11	0.0372 (6)	0.0212 (5)	0.0258 (5)	−0.0031 (5)	0.0000 (5)	0.0017 (4)
C12	0.0426 (7)	0.0297 (6)	0.0297 (6)	0.0054 (5)	0.0032 (5)	0.0013 (5)
C13	0.0597 (9)	0.0393 (7)	0.0351 (7)	0.0149 (7)	0.0094 (6)	0.0012 (5)
C14	0.0829 (12)	0.0400 (8)	0.0313 (7)	0.0077 (8)	0.0089 (7)	−0.0089 (6)
C15	0.0705 (10)	0.0422 (8)	0.0282 (6)	−0.0088 (7)	−0.0035 (6)	−0.0067 (5)
C16	0.0476 (7)	0.0286 (6)	0.0269 (5)	−0.0081 (5)	−0.0021 (5)	−0.0002 (4)
C17	0.0431 (7)	0.0407 (7)	0.0304 (6)	−0.0126 (6)	−0.0104 (5)	0.0020 (5)
C18	0.0316 (6)	0.0342 (6)	0.0330 (6)	−0.0087 (5)	−0.0044 (5)	0.0076 (5)
C19	0.0295 (6)	0.0566 (8)	0.0418 (7)	−0.0082 (6)	−0.0080 (5)	0.0138 (6)
C20	0.0242 (6)	0.0577 (9)	0.0523 (8)	0.0019 (6)	0.0020 (6)	0.0157 (7)
C21	0.0299 (6)	0.0487 (8)	0.0462 (7)	0.0008 (6)	0.0076 (6)	0.0009 (6)
C22	0.0264 (6)	0.0388 (7)	0.0347 (6)	−0.0036 (5)	0.0021 (5)	0.0002 (5)
C23	0.0283 (5)	0.0248 (5)	0.0294 (5)	−0.0054 (4)	−0.0014 (4)	0.0042 (4)

Geometric parameters (Å, º)

N2—C1	1.3263 (14)	C12—C13	1.3653 (17)
N2—C3	1.3924 (14)	C13—H13	0.9500
N9—H9	0.952 (13)	C13—C14	1.412 (2)
N9—C1	1.3653 (13)	C14—H14	0.9500
N9—C8	1.3816 (14)	C14—C15	1.350 (2)
C1—C10	1.4812 (14)	C15—H15	0.9500
C3—C4	1.3986 (16)	C15—C16	1.4301 (17)
C3—C8	1.4023 (15)	C16—C17	1.3869 (19)
C4—H4	0.9500	C17—H17	0.9500
C4—C5	1.3815 (17)	C17—C18	1.3876 (18)
C5—H5	0.9500	C18—C19	1.4290 (18)
C5—C6	1.4013 (18)	C18—C23	1.4389 (15)
C6—H6	0.9500	C19—H19	0.9500
C6—C7	1.3812 (17)	C19—C20	1.350 (2)
C7—H7	0.9500	C20—H20	0.9500
C7—C8	1.3968 (15)	C20—C21	1.4127 (19)
C10—C11	1.4196 (15)	C21—H21	0.9500
C10—C23	1.4152 (16)	C21—C22	1.3620 (18)
C11—C12	1.4296 (17)	C22—H22	0.9500

C11—C16	1.4390 (16)	C22—C23	1.4283 (16)
C12—H12	0.9500		
N2···C12	2.9836 (13)	C1···H12	2.61
N9···N2^{i}	2.8185 (12)	C1···H22	2.65
N9···C22	3.0403 (15)	C6···H21^{ii}	2.83
N2···H12	2.39	C7···H21^{ii}	2.78
H9···N2^{i}	1.918 (13)	C22···H9	2.784 (14)
N9···H22	2.47	H9···H22	2.28
H9···C1^{i}	2.778 (13)		
C1—N2—C3	105.51 (9)	C12—C13—H13	119.4
C1—N9—H9	128.7 (9)	C12—C13—C14	121.12 (14)
C1—N9—C8	107.15 (9)	C14—C13—H13	119.4
C8—N9—H9	124.2 (9)	C13—C14—H14	120.1
N2—C1—N9	112.34 (9)	C15—C14—C13	119.85 (12)
N2—C1—C10	124.05 (9)	C15—C14—H14	120.1
N9—C1—C10	123.59 (9)	C14—C15—H15	119.3
N2—C3—C4	130.47 (10)	C14—C15—C16	121.46 (13)
N2—C3—C8	109.27 (9)	C16—C15—H15	119.3
C4—C3—C8	120.24 (10)	C15—C16—C11	119.01 (12)
C3—C4—H4	121.2	C17—C16—C11	119.72 (11)
C5—C4—C3	117.70 (11)	C17—C16—C15	121.26 (12)
C5—C4—H4	121.2	C16—C17—H17	119.0
C4—C5—H5	119.3	C16—C17—C18	122.10 (11)
C4—C5—C6	121.40 (11)	C18—C17—H17	119.0
C6—C5—H5	119.3	C17—C18—C19	121.26 (11)
C5—C6—H6	119.1	C17—C18—C23	119.46 (11)
C7—C6—C5	121.88 (11)	C19—C18—C23	119.27 (11)
C7—C6—H6	119.1	C18—C19—H19	119.3
C6—C7—H7	121.7	C20—C19—C18	121.30 (12)
C6—C7—C8	116.59 (11)	C20—C19—H19	119.3
C8—C7—H7	121.7	C19—C20—H20	120.1
N9—C8—C3	105.72 (9)	C19—C20—C21	119.75 (12)
N9—C8—C7	132.11 (10)	C21—C20—H20	120.1
C7—C8—C3	122.17 (10)	C20—C21—H21	119.4
C11—C10—C1	118.95 (10)	C22—C21—C20	121.20 (13)
C23—C10—C1	120.53 (9)	C22—C21—H21	119.4
C23—C10—C11	120.51 (10)	C21—C22—H22	119.4
C10—C11—C12	123.76 (10)	C21—C22—C23	121.27 (12)
C10—C11—C16	118.89 (11)	C23—C22—H22	119.4
C12—C11—C16	117.33 (10)	C10—C23—C18	119.22 (10)
C11—C12—H12	119.4	C10—C23—C22	123.73 (10)
C13—C12—C11	121.15 (12)	C22—C23—C18	117.05 (11)
C13—C12—H12	119.4		
N2—C1—C10—C11	−46.69 (15)	C10—C11—C16—C17	2.15 (16)
N2—C1—C10—C23	134.18 (11)	C11—C10—C23—C18	−1.16 (16)

N2—C3—C4—C5	179.14 (11)	C11—C10—C23—C22	179.29 (10)
N2—C3—C8—N9	−0.86 (11)	C11—C12—C13—C14	−0.3 (2)
N2—C3—C8—C7	179.87 (10)	C11—C16—C17—C18	−0.14 (18)
N9—C1—C10—C11	131.47 (11)	C12—C11—C16—C15	2.81 (16)
N9—C1—C10—C23	−47.65 (15)	C12—C11—C16—C17	−176.28 (11)
C1—N2—C3—C4	−177.46 (11)	C12—C13—C14—C15	2.5 (2)
C1—N2—C3—C8	0.92 (11)	C13—C14—C15—C16	−2.0 (2)
C1—N9—C8—C3	0.46 (11)	C14—C15—C16—C11	−0.7 (2)
C1—N9—C8—C7	179.63 (12)	C14—C15—C16—C17	178.41 (13)
C1—C10—C11—C12	−2.26 (16)	C15—C16—C17—C18	−179.21 (12)
C1—C10—C11—C16	179.42 (9)	C16—C11—C12—C13	−2.37 (17)
C1—C10—C23—C18	177.95 (10)	C16—C17—C18—C19	176.68 (12)
C1—C10—C23—C22	−1.60 (16)	C16—C17—C18—C23	−2.53 (18)
C3—N2—C1—N9	−0.64 (12)	C17—C18—C19—C20	−179.47 (13)
C3—N2—C1—C10	177.71 (9)	C17—C18—C23—C10	3.16 (16)
C3—C4—C5—C6	0.28 (18)	C17—C18—C23—C22	−177.26 (11)
C4—C3—C8—N9	177.72 (10)	C18—C19—C20—C21	−2.4 (2)
C4—C3—C8—C7	−1.55 (16)	C19—C18—C23—C10	−176.07 (11)
C4—C5—C6—C7	−0.92 (19)	C19—C18—C23—C22	3.51 (16)
C5—C6—C7—C8	0.31 (18)	C19—C20—C21—C22	1.6 (2)
C6—C7—C8—N9	−178.15 (11)	C20—C21—C22—C23	1.8 (2)
C6—C7—C8—C3	0.91 (16)	C21—C22—C23—C10	175.24 (11)
C8—N9—C1—N2	0.12 (12)	C21—C22—C23—C18	−4.32 (17)
C8—N9—C1—C10	−178.24 (9)	C23—C10—C11—C12	176.86 (10)
C8—C3—C4—C5	0.91 (16)	C23—C10—C11—C16	−1.46 (16)
C10—C11—C12—C13	179.28 (11)	C23—C18—C19—C20	−0.26 (19)
C10—C11—C16—C15	−178.76 (11)		

Symmetry codes: (i) −*x*+3/2, *y*+1/2, *z*; (ii) *x*+1, *y*, *z*.

Hydrogen-bond geometry (Å, º)

*Cg*1, *Cg*2, *Cg*3 and *Cg*4 are the centroids of the (N2/N9/C1/C3–C8), (C10/C11/C16–C21), (C10/C11/C16–C18,C23) and (C3–C8) rings, respectively.

D—H···*A*	*D*—H	H···*A*	*D*···*A*	*D*—H···*A*
N9—H9···N2^{i}	0.95 (1)	1.92 (1)	2.8186 (13)	157 (1)
C5—H5···*Cg*1^{iii}	0.95	2.96	3.8219 (12)	151
C13—H13···*Cg*2^{iv}	0.95	2.97	3.4156 (14)	110
C20—H20···*Cg*3^{i}	0.95	2.90	3.5625 (16)	128
C21—H21···*Cg*4^{v}	0.95	2.75	3.2887 (15)	116

Symmetry codes: (i) −*x*+3/2, *y*+1/2, *z*; (iii) *x*+1/2, *y*, −*z*+3/2; (iv) −*x*+3/2, *y*−1/2, *z*; (v) *x*−1, *y*, *z*.